Materials Characterization 137 (2018) 1–8

Contents lists available at ScienceDirect

Materials Characterization

journal homepage: www.elsevier.com/locate/matchar

Microstructure control to improve creep strength of alumina-forming austenitic heat-resistant steel by pre-strain

Min-Ho Jang[a,b], Jun-Yun Kang[b], Jae Hoon Jang[b], Tae-Ho Lee[b,*], Changhee Lee[a,*]

[a] Division of Materials Science and Engineering, Hanyang University, Seongdong-ku, Seoul 133-791, Republic of Korea
[b] Ferrous Alloy Department, Advanced Metallic Materials Division, Korea Institute of Materials Science, 797 Changwondaero, Seongsangu, Changwon, Gyeongnam 642-831, Republic of Korea

ARTICLE INFO

Keywords:
Creep test
Pre-strain
Precipitation behavior
Alumina-forming austenitic heat-resistant (AFA) steel

ABSTRACT

At 700 °C and 200 MPa, the creep rupture time of W-containing alumina-forming austenitic heat-resistant (WAFA) steel increases from 1044 to 3119 h by pre-strain. Pre-strain introduces a lot of dislocation into the matrix and most of the dislocations remain stable to the end of creep without recovery and recrystallization. In addition, the dislocations have enabled secondary NbC and Laves phase to be uniformly distributed and refined. However, the dislocations lower grain boundary strength due to the coarsening of precipitates along grain boundaries Therefore, the increase in the creep rupture time in spite of deterioration of grain boundary strength is attributed to the dislocation strengthening and enhanced precipitation hardening within grains.

1. Introduction

The influence of pre-strain on the creep strength of heat-resistant alloys has been the focus of many studies in recent years since a thermal power plant inevitably requires many U-bending parts among the steam tubes, in which a considerable amount of pre-strain occurs during fabrication processing due to the structural geometry [1–5]. In Ni-based alloys, the pre-strain reduces the creep strength because the grain-boundary cavities tend to form easily due to the increase in mobile dislocations [1–2]. In 347 austenitic stainless steel, a typical austenitic stainless steel used in parts of steam tubes, the precipitation of the detrimental sigma phase is accelerated due to deformation twins induced by pre-strain, which reduce the creep strength [3]. However, pre-strain has been reported to have a positive effect in higher 20 Ni austenitic heat-resistant steels [4,5]. Saito and Komai reported that pre-strain improves the creep strength of 25Cr20NiNbN steel because a high density of dislocations is maintained until the late stage of creep at 650 °C. On the other hand, when tested at temperatures over 700 °C, the creep strength of the pre-strained steels were deteriorated because of agglomeration and coarsening of precipitates as well as the recovery of dislocations [4]. Alumina-forming austenitic heat-resistant steel (14Cr-20Ni-2.5Al-Nb, AFA steel) showed improved creep strength by pre-strain even above 700 °C [5]. Yamamoto et al. asserted that pre-strain introduced dislocations, acting as nucleation sites for the precipitation of hardening phase, which improved creep strength [5]. However, systematic research has been hardly conducted on this phenomenon and the evidence for it is insufficient [5–9]. H.H. Park et al. also argued that pre-strain in the AFA steels improves creep strength [10], but it is difficult to cover the failure analysis in the U-bending part because the amount of pre-strain is lited to about 5%. Therefore, it is necessary to investigate in detail how pre-strain affects creep properties and microstructure when a large amount of pre-strain (i.e. 30%) is applied.

After considering the factors above, we can predict that pre-strain can help improve creep strength in the dislocation creep region if the dislocations introduced by pre-strain are maintained until the end of creep, and if microstructural degradation such as coarsening and sigma phase formation can be suppressed. AFA steels have a high Nb content (approximately 0.9 wt%), which enhances precipitation hardening through the formation of fine, uniformly-distributed secondary NbC and Laves phases (Fe2M, M = Mo, Nb and W) [5–9]. It has been shown that the secondary NbC can suppress the movement of dislocations and sub-boundaries during hot compression at elevated temperatures [11]. In addition, AFA steel showed the coarsening of precipitates and the precipitation of sigma phase at 700 °C and 160 MPa, but these can be retarded by the addition of W [12]. In this study, we systematically study the reason why pre-strain improves creep strength in AFA steels and establish the conditions required for creep strength to be improved by pre-strain.

2. Experimental Procedures

Table 1 shows the chemical composition (in wt%) of the W-

* Corresponding authors.
E-mail addresses: jmhaos@kims.re.kr (M.-H. Jang), Firice@kims.re.kr (J.-Y. Kang), jhjang@kims.re.kr (J.H. Jang), lth@kims.re.kr (T.-H. Lee), chlee@hanyang.ac.kr (C. Lee).

https://doi.org/10.1016/j.matchar.2018.01.005
Received 4 September 2017; Received in revised form 3 January 2018; Accepted 3 January 2018
Available online 04 January 2018
1044-5803/

Table 1
Chemical composition of WAFA steel (wt%).

wt%	C	Si	Mn	Al	Cr	Ni	Mo	W	Nb	B	P
WAFA	0.084	0.152	1.915	2.567	14.02	19.837	0.887	3.697	0.854	0.011	0.011

containing AFA (WAFA) steel. This steel was prepared from commercially pure elements and was fabricated using a vacuum induction melting furnace (VIM 4 III-P; ALD Vacuum Technologies, Germany). The ingot was homogenized at 1250 °C for 2 h. After homogenization, the ingot was hot- (1000 °C) and cold-rolled to a total thickness reduction of 80%. The cold-rolled steel was solution-treated at 1250 °C for 1 h and water quenched. The equilibrium phase fraction of the investigated steel was calculated using the MatCalc (database mc_fe 2.045). Specimens with pre-strain (prestrained steel) were subjected to 30% elongation using a commercial tensile machine (Instron 5882, Instron Corporation, Canton, MA). The specimen geometry for forward creep tests was designed according to the ASTM standard E8. The creep properties of the alloys were obtained in air at 700 °C and 200 MPa using a creep testing machine (Series 2320 lever arm creep, Applied Test Systems, USA). Elongation of the gauge length was measured using a linear variable differential transformer (LVDT) attached to an extensometer. The creep specimens had a cylindrical shape with a diameter of 6 mm and a gauge length of 25 mm. Some of the specimens were aged at 700 °C for up to 504 h to examine the microstructural evolution and then water quenched. Microhardness of the specimens was measured on the polished surface at 1 kgf loads using a microhardness tester (FM-700; Future tech. Corp., Japan). The microstructures of the creep and aged samples were observed using an optical microscope (OM), a field-emission scanning electron microscope (FE-SEM; JSM-7001F, JEOL), a transmission electron microscope (TEM; JEM-2100F, JEOL), and a spherical aberration corrected (Cs) field-emission transmission electron microscope (HR-TEM; JEM-2100F/CESCOR, JEOL, Japan).

Kernel average misorientation (KAM) map was obtained using electron backscatter diffraction (EBSD) analysis. The samples for OM and SEM observations were mechanically polished and were prepared without etching to protect the precipitates of the creep tested and aged samples. The thin foils for TEM were prepared by twin-jet electrolytic polishing using a mixed solution of 10% perchloric acid and 90% methanol at − 25 °C at an applied potential of 20.5 V. The volume fraction and size of the second phases were measured using image analysis (ImageJ software).

3. Results

3.1. The Equilibrium Phase Diagram and Initial Microstructures before Creep

The equilibrium phase diagram of the investigated alloy is drawn in Fig. 1. The equilibrium microstructure after solution treatment at 1250 °C showed austenite matrix with primary NbCs which could be not dissolved at that temperature. It is conceivable that a second phase such as NiAl, Laves and secondary NbC would form during creep at the aging temperature (700 °C). Shown in Fig. 2 is the solution-treated microstructure of WAFA (unstrained steel) consisting of an austenite matrix with coarse particles which are identified as the primary NbC using TEM analysis together with SADP (selected area diffraction pattern) and EDS (energy dispersive X-ray spectroscopy) in Fig. 2 (b, d). Therefore, the solution treated microstructure of unstrained steel matches well with the results of the thermodynamic calculations in Fig. 1. However, an unexpected number of dislocations were present within matrix, and characterized by individual dislocations, dislocation tangles and planar structure as shown in Fig. 2 (c). The dislocations, which were formed during cold rolling and quenching, were not completely recovered or recrystallized after solution treatment. This is because the AFA steels are slower to recrystallize and recover fine secondary NbC than other stainless steels [11]. In particular, planar structures are well developed along the {111} slip system, and these dislocation structures are similarly found in austenitic stainless steel such as Sancro25 and 316 L [13,14].

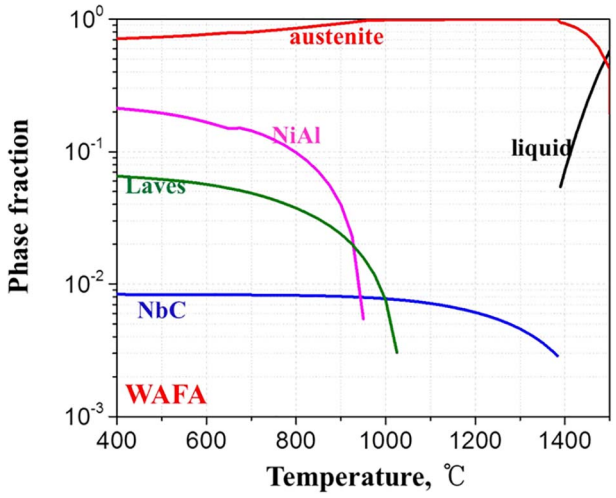

Fig. 1. Equilibrium phase fraction of investigated steel calculated using MatCalc.

The microstructure of the steel with pre-strain (prestrained steel) is quite different from that of the unstrained steel, as shown in Fig. 3. The microstructure of prestrained steel is elongated along the direction of the tensile stress and also primary NbCs were formed. Compared with planar dislocation structure in unstrained steel, it is noted that dislocation structure is characterized by a typical dislocation cell structure with high density and dislocation tangles. This deformation behavior of WAFA steel can be explained in terms of stacking fault energy (SFE) because the deformation behavior of austenitic steel strongly depends on the SFE [15]. It is well known that the deformation mode gradually changes in sequence from strain-induced matensitic transformation (SIMT), to deformation twin (DT), to dislocation glide or dislocation cell in proportion to SFE. The SFE in austenitic steel is simply expressed in terms of chemical composition [16]:

$$\text{SFE}\ (\text{mJ/m}^2) = -53 + 6.2[\text{Ni}] + 0.7[\text{Cr}] + 3.2[\text{Mn}] + 9.3[\text{Mo}] \quad (1)$$

where [X] represents the weight percent in austenitic steel of each element. The SFE of 347 austenitic stainless steel, which results in deformation twinning during plastic deformation, is 20.59 mJ/m^2 [17]. The SFE of WAFA steel in this study is estimated to be 94.14 mJ/m^2 due to a higher Ni content than 347 stainless steel, and so the formation of dislocation cells in Fig. 3 (b, c) can be also explained by the difference in SFE. In unstrained steel, most of the dislocations, formed by hot and cold rolling, is recrystallized or recovered during solution treatment and a few dislocations such as planar dislocation are left.

3.2. Creep Properties and Microstructure after Creep

The creep rupture test was conducted at 700 °C under the applied stress of 200 MPa and the rupture times (t_r) of unstrained and pre-strained steels were 1044 and 3119 h, respectively, as shown in Fig. 4 (a). The minimum creep rate decreased from 6.78×10^{-4} to 3.54×10^{-4} after pre-strain. The amount of creep strain and the strain